Journal of Power Sources 247 (2014) 572–578

Contents lists available at ScienceDirect

Journal of Power Sources

journal homepage: www.elsevier.com/locate/jpowsour

Durability of nickel–metal hydride (Ni–MH) battery cathode using nickel–aluminum layered double hydroxide/carbon (Ni–Al LDH/C) composite

Alexis Bienvenu Béléké [a], Eiji Higuchi [b], Hiroshi Inoue [b], Minoru Mizuhata [a, *]

[a] Department of Chemical Science & Engineering, Graduate School of Engineering, Kobe University, 1-1 Rokko, Nada, Kobe 657-8501, Japan
[b] Department of Applied Chemistry, Graduate School of Engineering, Osaka Prefecture University, Sakai, Osaka 599-8531, Japan

HIGHLIGHTS

- We report the durability of the optimized Ni–Al LDH/C as cathode materials.
- We evaluate the performance at 5.0 and 5.8 mA for a total number of 869 cycles.
- The electrode maintains the capacity retention above 380 mA h g_{comp}^{-1}.
- A higher current regime is beneficial in terms of materials utilization.
- The α-Ni(OH)$_2$/γ-NiOOH redox reaction occurs without any intermediary phase.

GRAPHICAL ABSTRACT

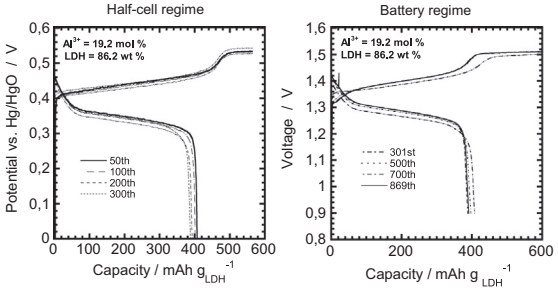

ARTICLE INFO

Article history:
Received 28 March 2013
Received in revised form
27 June 2013
Accepted 1 August 2013
Available online 11 September 2013

Keywords:
Active materials
Positive electrode
Layered double hydroxide
Ni–MH batteries

ABSTRACT

We report the durability of the optimized nickel–aluminum layered double hydroxide/carbon (Ni–Al LDH/C) composite prepared by liquid phase deposition (LPD) as cathode active materials in nickel metal hydride (Ni–MH) secondary battery. The positive electrode was used for charge–discharge measurements under two different current: 5 mA for 300 cycles in half-cell conditions, and 5.8 mA for 569 cycles in battery regime, respectively. The optimized Ni–Al LDH/C composite exhibits a good lifespan and stability with the capacity retention above 380 mA h g_{comp}^{-1} over 869 cycles. Cyclic voltammetry shows that the α-Ni(OH)$_2$/γ-NiOOH redox reaction is maintained even after 869 cycles, and the higher current regime is beneficial in terms of materials utilization. X-ray diffraction (XRD) patterns of the cathode after charge and discharge confirms that the α-Ni(OH)$_2$/γ-NiOOH redox reaction occurs without any intermediate phase.

© 2013 Elsevier B.V. All rights reserved.

1. Introduction

The increasing demands of mobile electronics in today's society set up scientists to an imperious challenge to improve existing battery technologies and/or to develop new materials in order to achieve high energy density, high power density and low cost rechargeable batteries. Despite the progress in lithium chemistry, nickel metal-hydride (Ni–MH) battery still finds applications in other areas such as power assist bicycles, power tools, and hybrid electric vehicles (HEVs) [1,2]. In Japan, the high large-scale capacity and fully sealed Ni-MH battery pack, GIGACELL developed by Kawasaki Heavy Industries (KHI), Ltd. is considered as the next generation battery energy storage due to its wide range of applications including streetcars (battery driven light rail vehicle (LRV)), power system for railways, backup power source, forklift truck, electric vehicles (EVs), transfer crane and elevators. GIGACELL is also

* Corresponding author.
E-mail address: mizuhata@kobe-u.ac.jp (M. Mizuhata).

0378-7753/$ – see front matter © 2013 Elsevier B.V. All rights reserved.
http://dx.doi.org/10.1016/j.jpowsour.2013.08.001

compatible with wind power plants or photovoltaic system [3a,b]. In this scope, Takasaki et al. have recently prepared a fiber-type nickel-hydroxide electrodes by the electrodeposition of pure nickel hydroxide $Ni(OH)_2$ on nickel-plated carbon fibers [4]. Their Ni–MH test cells containing the fiber-type $Ni(OH)_2$ electrodes exhibited good electrode performances, such as a 300 mA h/g large discharge capacity, 2000 long cycle-life and high-rate charge/discharge even at the 100–500 C rates. Despite such high performances, the authors have observed a degradation of the electrochemical reactivity of their fiber-type $Ni(OH)_2$ electrode due to the effects of CoOOH coating. Furthermore, their electrodes suffer from high volume expansion which affected the cycle-life. These are the principal limitations of pure $Ni(OH)_2$ as active materials for the positive electrode in commercial nickel rechargeable batteries.

According to the Bode general reaction scheme [5] (see Supporting information (1) for illustration) elucidated below;

it is clear that the electrochemical cycling of the positive electrode of Ni batteries takes place between β(II)-$Ni(OH)_2$ and β(III)-NiOOH phases. These two materials exhibit a layer structure made of NiO_2 sheets, between which protons are intercalated. Both phases crystallize in hexagonal system, the *c* parameter, corresponding to the intersheet distance, is equal to 4.6 Å for the reduced β(II) phase and to 4.7 Å for the oxidized phase β(III). After a strong overload of the cell or a long period of floating, a γ-type phase with an expanded *c* parameter of 7 Å may be formed; then after the cell discharge, the β(II) phase is recovered. The repetition of such a process results in considerable damage to the nickel oxide electrode as a result of mechanical deformation.

From a theoretical point of view, the $\alpha \leftrightarrow \gamma$ cycling which appears on this diagram exhibits several advantages compared with the $\beta \leftrightarrow \gamma$ cycling: (i) a large number of electron exchanged per nickel atom, as the oxidation state of nickel in γ-NiOOH can reach 3.6 ± 0.1 [6], (ii) a decrease in the mechanical deformation resulting from the suppression of the $\beta(II) \rightarrow \gamma$ reaction, and (iii) a higher diffusion coefficient for the proton due to the presence of the layer water molecules between NiO_2 slabs [7]. It is therefore desirable for nickel batteries to have only the $\alpha \leftrightarrow \gamma$ cycling. However, α-$Ni(OH)_2$ is difficult to prepared and unstable in alkaline media because it easily reverts to β-$Ni(OH)_2$. Several studies have been carried out through partial substitution of some fractions of Ni^{2+} ions with trivalent metal additives including aluminum, cobalt, iron, manganese, zinc and chromium in the lattice of the α-$Ni(OH)_2$ for its stabilization [8–14]. Among these metals, Al is considered as the best additive due to its good stability [9]. Many works on the preparation of Al-substituted α-$Ni(OH)_2$ (also called nickel–aluminum layered double hydroxide (Ni–Al LDH)) using different techniques have been reported [9,15,16].

In our previous reports, we have developed a novel technique of preparation of Ni–Al LDH/C composite for battery applications, the so-called liquid phase deposition (LPD) method. LPD is one of the *chimie douce* techniques of preparation of metal oxide thin films developed by Nagayama et al. [17] and Hishinuma et al. [18], It has been pioneered by Deki's group for the past two decades [19–22]. Its basic concept is described elsewhere and the main reactions can be expressed as follows:

$$MF_x^{(x-2n)^-} + nH_2O = MO_n + xF^- + 2nH^+ \quad (2)$$

$$H_3BO_3 + 4HF = BF_4^- + H_3O^+ + 2H_2O \quad (3)$$

$$Al + 6HF = H_3AlF_6 + 3/2H_2 \quad (4)$$

In the conventional LPD process, the hydrolysis reaction of the metal-fluoro complex, Eq. (2) is followed by addition of either boric acid (H_3BO_3), Eq. (3) or aluminum metal Eq. (4) which acts as a fluoride scavenger. The role of boric acid is not only to serve as fluoride scavenger, but it also shifts reaction (2) to the right side by producing water. For the preparation of Ni–Al LDH, Eqs. (2), (3) and (5) were applied in which $Al(NO_3)_3$ Eq. (5) serves as a trivalent additive metal for the substitution of Ni^{2+} cations in the $Ni(OH)_2$ lattice.

$$Al(NO_3)_3 + 6HF = H_3AlF_6 + 3HNO_3 \quad (5)$$

Once the oxide's solubility limit is reached, homogeneous nucleation occur, and thin films are formed by crystal and random structured oxide layer from the substrate and the oxide layer grows onto the substrate.

In this context, the LPD offers the possibility to control the amount of Ni^{2+} cations substituted by Al^{3+} cations within the $Ni(OH)_2$ lattice, the amount of the resulting films deposited over carbon particles, as well as other advantages such as phase purity, crystallinity and no pH adjustment.

In our previous works, we have discussed the viability of the LPD method and evaluated the performance of Ni–Al LDH/C composite as cathode active materials in battery regime [23,24]. We have also improved our synthetic route and found that the optimized Ni–Al LDH/C composite results in high performance cathode materials in half cell conditions [25]. More recently, Mizuhata's group has studied the anion exchange properties of Ni–Al LDH prepared by the LPD method [26]. In this study, we investigate the durability of the optimized Ni–Al LDH/C cathode materials containing 19.2 Al mol% and 86.2 wt% LDH in both half-cell and battery regime, respectively. The electrochemical properties of the electrode are evaluated by charge–discharge and cyclic voltammetry measurements, respectively. The structural changes undergone by the cathode after oxidation (charging of the Al-substituted α-$Ni(OH)_2$), and after discharge are characterized by X-ray diffractions (XRD).

2. Experimental

2.1. Materials and preparation

2.1.1. Carbon oxidation

Carbon black with 50 nm of primary average diameter and 50 $m^2\ g^{-1}$ of the specific surface area was used as a conductive agent. It was oxidized using $KMnO_4$ aqueous solution as follow: 2.0 g of carbon black was first loaded in a bottomed flask set under refrigerant. Then 15.986 g of $KMnO_4$ was dissolved into 200 mL deionized water by hot stirring for a few minutes, and loaded into a 500 mL mesh cylinder. Next, 132 mL of 4 M ($M = mol\ dm^{-3}$) HNO_3 solution was added on the $KMnO_4$ solution. The amount of the mixture was adjusted with deionized water to make 400 mL solution which was poured on carbon black contained in the bottomed flask. The system was mixed by stirring at 70 °C for 4 h under refrigerant, filtrated and washed with hot deionized water three times. The filtrate was shaken again in 400 mL of 2 M HCl for 17 h at an ambient temperature, washed with hot deionized twice, and dried at 110 °C for 8 h.

2.1.2. Nickel parent solution

The Ni parent solution was prepared as follows: 120 g of $Ni(NO_3)_2 \cdot 6H_2O$ (Nacalai Tesque Inc.) were dissolved into 800 mL of ion exchange water and, while keeping under stirring, ca. 50 mL of 33 vol% of aqueous NH_3 (Nacalai Tesque Inc.) was drop-wisely added until pH reached 7.5. The collected precipitate was repeatedly washed with deionized water and dried at ambient temperature. It was then agitated into 750 mL of 0.66 M NH_4F (Nacalai Tesque Inc.) for 48 h at ambient temperature, and filtered to give Ni parent solution.

2.1.3. Reaction solution

The reaction solution consisted of the abovementioned Ni parent solution (30 mM Ni^{2+} in 0.66 M NH_4F), 40 mL of 0.5 M aqueous H_3BO_3 and 4.8 mL of 50 mM aqueous $Al(NO_3)_3$, respectively, mixed and diluted with deionized water. The final concentration of Ni^{2+}, H_3BO_3 and $Al(NO_3)_3{\cdot}9H_2O$ in the reaction solution was 12 mM, 0.1 M and 1.2 mM, respectively, giving $Al^{3+}/Ni^{2+} = 10$ mol% and $Al^{3+}/(Al^{3+}+Ni^{2+}) = 9$ mol%.

2.1.4. Composite preparation

Ni–Al LDH/C composite was prepared according to the optimized procedure: 20 mg oxidized carbon was loaded in a plastic polypropylene bottle. Therein 200 mL of the reaction solution were added. The mixture was shacked ultrasonically until carbon particles are completely dispersed. The bottle was then placed in a water bath at 50 °C for 48 h to form Ni–Al LDH loaded carbon. The resulting Ni–Al LDH/C was collected by suction filtration, washed repeatedly with hot deionized water and dried at 50 °C for 3 h. Finally, a Ni–Al LDH/C composite containing 86.2 wt% of LDH/carbon ratio (LDH content) and 19.2 mol% of $Al^{3+}/(Ni^{2+} + Al^{3+})$ cation was obtained.

2.2. Composite characterization

The concentrations of Ni^{2+} and Al^{3+} in the Ni–Al LDH/C composite or parent solution were determined by inductively coupled plasma–atomic emission spectroscopy (ICP-AES, HORIBA Ltd., ULTIMA 2000). Five milligrams of the composite was ultrasonically dispersed in 50 cm^3 of diluted HNO_3 solution (0.26 M), and stored in the oven at 50 °C for 48 h to allow dissolution of Ni^{2+} and Al^{3+}. The dispersion was then filtrated to remove carbon, and the filtrate was used as sample for the ICP-AES measurements. The crystalline structures of the composites were characterized using an X-ray diffractometer (Rigaku RINT-TTR/S2).

2.3. Cell fabrication and electrochemical tests

The positive electrode was fabricated as follows: 6.7 mg of the Ni–Al LDH/C composite (containing 5.77 mg of LDH) was mixed with 20 mg of 2 g cm^{-3} polyvinyl alcohol (PVA) aqueous solution as a binder to make a paste. The resulting paste was loaded into a 1×1 cm^2 nickel foam, dried under vacuum at 80 °C for 1 h, then pressed at 20 MPa for 1 min using a programmed digital press (Shinto Digital Press, Japan). The negative electrode was constructed in a same way as the positive electrode. 100 mg of hydrogen storage alloy powder provided by Kawasaki Heavy Industries, Akashi, Japan was mixed with 44.4 $\times$ 10^{-6} dm^3 of PVA solution to make a paste. The paste was loaded into a 2×1.5 cm^2 nickel foam, dried under vacuum at 120 °C for 1 h, and pressed under 118 MPa for 1 min. The Hg/HgO into 6 M KOH was employed as the reference electrode while 6 M KOH solution served as an electrolyte solution.

Charge–discharge measurements were performed using a potentiostat (HOKUTO DENKO HZ5000, Japan) while cyclic voltammetry was carried out using a Solartron SI 1287 Electrochemical Interface at a scan rate of 1 mV s^{-1} versus Hg/HgO after all charge–discharge tests. The cell was immersed into 6 M KOH at open circuit voltage for 3 days for conditionings to allow anions exchange between extra ions and OH^-. The electrolyte solution was deaerated by argon bubbling for 15 min prior to measurements. It was then activated by charging and discharging at the 5.0 C-rate for 50 cycles. The durability test of the positive electrode was evaluated in two steps under different currents: 5.0 mA and 5.8 mA, respectively. These two currents were calculated based on the weight of the active material (5.77 mg), the time (0.5 h = 30 min) and the theoretical capacity of α-$Ni(OH)_2$ (433 mA h g^{-1}) described below:

$$\text{Capacity} = \frac{\text{Current(mA)*time(h)}}{\text{weight(g)}} \quad (6)$$

The applied current of 5.0 mA corresponds to 100% while that of 5.8 mA corresponds to 116%, of the α-$Ni(OH)_2$ theoretical capacity [27]. The purpose of overcharging the battery at a high current was to check the electrochemical stability of our materials.

The cell was charged at 5.0 mA (866.5 mA g^{-1}) for 30 min and discharged to 0 V for 300 cycles vs Hg/HgO in half cell conditions. It was allowed to rest for 15 h before being submitted to cyclic voltammetry tests. Thereafter, the same cell was charged again at 5.8 mA (1005 mA g^{-1}) for 30 min in battery regime, and discharged to 0.9 V for 569 more cycles.

For the investigation of the crystalline structure of the positive electrode after charge–discharge, two electrodes of the same batch of Ni–Al LDH/C composite were fabricated. For each of them, 50 mg of Ni–Al LDH/C composite was mixed with 300 μL of 2% PVA to make a paste. The paste was loaded into a 2×2 cm^2 nickel foam. Another 2×2 cm^2 nickel foam was used as counter electrode. Ag/AgCl in saturated KCl served as reference electrode while 6 M KOH was employed as the electrolyte solution. Galvanostatic charge–discharge measurements were operated on Voltalab (Radiometer Analytical S.A., PGZ402). The experiments were carried out under half cell conditions according to the same procedure as described in Ref. [24]. After each test, the electrode was removed from the electrolyte and disconnected from the current collector. Nickel foam containing Ni–Al LDH/C composite after charge–discharge tests was rinsed with deionized water, opened from the top edge, and dried in an oven at 50 °C for 2 h before XRD characterization.

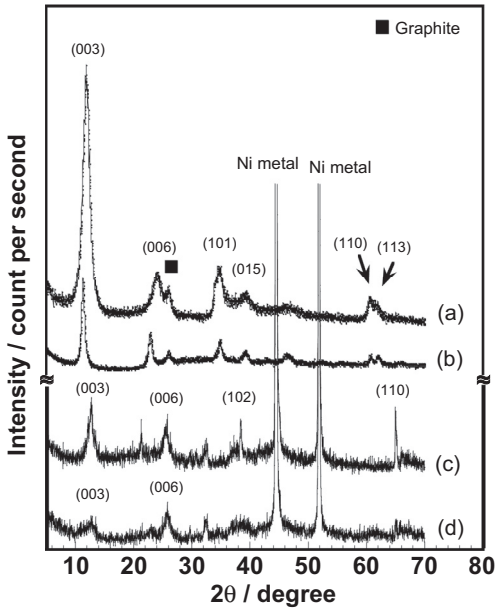

Fig. 1. XRD patterns of Ni–Al LDH/C composite: (a) as-dep α-$Ni(OH)_2$, (b) α-$Ni(OH)_2$ after conditionings (before charge), (c) γ-NiOOH obtained after oxidation of α-$Ni(OH)_2$, (d) α-$Ni(OH)_2$ after charge–discharge.

3. Results and discussion

3.1. Composition and structure

XRD patterns of the Ni–Al LDH/C composite at different stages of measurements are shown in Fig. 1. The corresponding numerical

Table 1
(003) and (006) diffractions data of Ni–Al LDH/C composite before and after different stages of measurements.

Diffractions			As-dep (α-Ni(OH)$_2$)		After conditionings α-Ni(OH)$_2$		After charge (γ-NiOOH)		After discharge (α-Ni(OH)$_2$)	
h	*k*	*l*	$2\theta_{obs}$(°)	*d* (Å)	$2\theta_{obs}$(°)	*d* (Å)	$2\theta_{obs}$(°)	*d* (Å)	$2\theta_{obs}$(°)	*d* (Å)
0	0	3	11.95	7.39	11.35	7.79	12.76	6.92	12.68	6.97
0	0	6	24.03	3.69	22.84	3.88	25.84	3.44	25.80	3.45

values of the major diffractions (003) and (006) are summarized in Table 1. The as-deposited sample (Fig. 1a) shows the same diffraction characteristics to Ni–Al LDH [8,23–26], isostructural to α-Ni(OH)$_2$·0.75H$_2$O (JCPDS card # 38-715). Fig. 1b presents an XRD pattern of the composite after three days immersion in 6.0 M KOH, corresponding to the structure of the active materials after the conditionings (before charge). This diffraction pattern displays similar characteristics to that of the as-deposited sample except that it shows narrow, sharp and more symmetrical peaks. Furthermore, the peak positions of the major diffraction planes (003) and (006) shift toward lower 2 theta values, indicating an increasing of the interlayer distance. These information imply that some structural modifications have occurred during KOH treatment, leading to a more ordered structure [28]. Fig. 1c depicts diffraction pattern for the electrode after charging (oxidation of the Al-substituted α-Ni(OH)$_2$). These features could be indexed as a typical structure of γ-NiOOH according to the JCPDS card # 6-0075 [29,30]. Fig. 1d shows an XRD pattern for the electrode obtained after discharge. The intensities of the mayor diffraction planes (003) and (006) are very weak due to the highest intensity of Ni metal diffraction, and also because that only a few amount of active materials could be detected by the X-rays. Although the peak positions are closer to that of γ-NiOOH, there are assigned to α-Ni(OH)$_2$ (JCPDS card # 38-715). The most important point is that no peak for β-Ni(OH)$_2$ or β-NiOOH is observed, indicating that the electrochemical reactions take place without any intermediate phase [31]. The high intensity of the (003) peak of the as-deposited sample indicates that the composite prepared under this conditions possesses a high crystallinity [28] due to the optimized amount of the composition ratio between LDH and carbon particles. On the other hand, the numerical values of the XRD patterns in Table 1 clearly show the variation of the peak positions of d_{003} and d_{006} in Fig. 1a–c. The peak positions of these two diffractions shift from 7. 39 Å and 3.69 Å for the as-prepared samples (Fig. 1a) to 7. 79 Å and 3.88 Å, respectively, after conditioning (Fig. 1b). Upon charging, they decrease to 6.92 Å and 3.44 Å due to the phase transformation from α- to γ-form (Fig. 1c). After discharge, they slightly shift to 6.97 Å and 3.45 Å, respectively (Fig. 1d), much closer to those of γ-NiOOH. This result confirms that the α/γ phase transformation occurs with no mechanical deformation [32].

The increase of d_{003} and d_{006} from 7. 39 Å and 3.69 Å to 7. 79 Å and 3.88 Å, respectively in the XRD patterns between the as-prepared samples and the electrode before charging is caused by the structural rearrangements that have occurred during conditionings. The main purpose of the conditionings is to allow an exchange of extra anions in the gallery of the LDH with OH^-. In such a circumstance, a typical α-type or a Al-substituted α-Ni(OH)$_2$ with a low $Al^{3+}/(Al^{3+} + Ni^{2+})$ content would have been converted into β-type (see Supporting information (2)). Infrared studies in our previous work have shown that the as-deposited composite contains an excess of anions such as bound nitrates ion in C_{2v} symmetry as well as the probability of the presence of tetrafluoroborates (BF_4^-) and/or tetrafluoroaluminates (AlF_4^-) adsorbed on the external surface of the crystallinities, since they are involved in the reaction mechanism of the deposition in the LPD process [24]. Upon KOH treatment, these extra anions are exchanged with OH, leaving only free nitrate ions in D_{3h} symmetry and water molecules in the gallery. The removal of these extra anions leads to a rearrangement of the structure including some variation of the interlayer distance of the (003) and (006) diffractions. Hu et al. have observed that the (003) diffraction of their LDH shifts toward a higher 2θ value after being treated in alkali solution for 1 day [31]. Hengbin and co-workers have found the same behavior for their Ni–Al LDH prepared by direct titration method [32].

3.2. Charge–discharge

Typical charge–discharge curves of the 50th, 100th, 200th and 300th cycles of the cell at 5.0 mA are shown in Fig. 2. The electrode displays the same features throughout all the cycles. On the charging, a low polarization and a slow oxygen evolution are observed for the 200th cycle while on discharging, a higher discharge potential plateau with high discharge capacity can be observed for the 50th cycle. The evolution of the discharge capacity over 300 cycles is depicted in Fig. 3. The discharge capacity evolves in two steps: at first, it significantly increases from 348 to 408 mA h g_{LDH}^{-1} from the beginning up to the 50th cycle, which corresponds to the activation period, then gradually decreases to 388 mA h g_{LDH}^{-1} at the 300th cycle. Such discharge capacity indicates that the number of exchanged electron (NEE) per Ni atom in a gram of composite varied between 1.34 and 1.41 during the cycles. Despite a fading of 4.9%, the discharge capacity is maintained above 380 mA h g_{LDH}^{-1}.

Fig. 4 shows charge–discharge curves of the battery at 5.8 mA for the 301st, 500th, 700th and 869th cycles, respectively. The cell exhibits same features throughout all the cycles with a nominal voltage of 1.56 V, which corresponds to an enhancement of 20% of current commercial Ni–MH secondary battery. On charging, the 301st cycle shows a much lower polarization and a slower oxygen evolution compared to other cycles. On the discharge, it can be

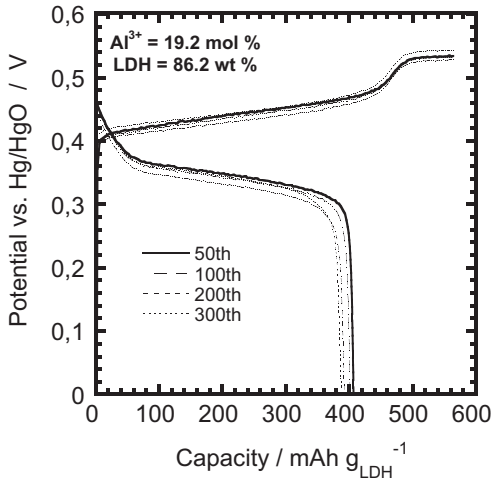

Fig. 2. Charge–discharge curves at 5.0 mA (2.0 C-rate) for the 50th, 100th, 200th and 300th cycles.

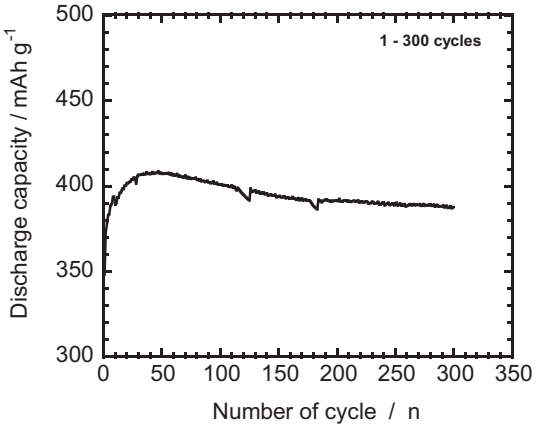

Fig. 3. Evolution of the discharge capacity at 5.0 mA (2.0 C-rate) for 300 cycles. There are some ripping and waves due to technical sources. During these experiments, operations for measurement were stopped and resumed again after few hours.

noticed that the cell maintains an excellent discharge behavior throughout all the cycles. More importantly, the 869th cycle shows the highest discharge voltage plateau lying between 1.3 and 1.26 V. The evolution of the discharge capacity from the 301st to the 869th cycles is plotted in Fig. 5. The discharge capacity starts at 404 mA h g_{LDH}^{-1} from the 301st, drops to 387 mA h g_{LDH}^{-1} around the 380th cycle. It increases to 397 mA h g_{LDH}^{-1} around the 500th cycle, remains constant up to the 580th cycle and finally slightly decreases to end up at 389 mA h g_{LDH}^{-1}. The minimum discharge capacity attained during these 869 cycles is as high as 388 mA h g_{LDH}^{-1}, which corresponds to a minimum number of exchanged electrons of 1.34 per Ni atom per gram of composite. The high capacity retention in a long cycle-life over 800 cycles is mainly attributed to the good crystallinity of the composite after an optimization of the synthetic procedure. Two parameters are crucial to achieve Ni–Al LDH/C composite with a good crystallinity: (i) the cationic ratio $Al^{3+}/(Al^{3+} + Ni^{2+})$ in the α-$Ni(OH)_2$ lattice, and (ii) the LDH/carbon ratio (LDH content). Controlling these parameters is the key point to superior electrochemical performance. This result is in a good agreement with our previous report [25] and also consistent with the literature [33–38]. It points out that Ni–Al LDH/C composite prepared by LPD method can be employed as high discharge rate electrode materials for Ni–MH rechargeable batteries [39].

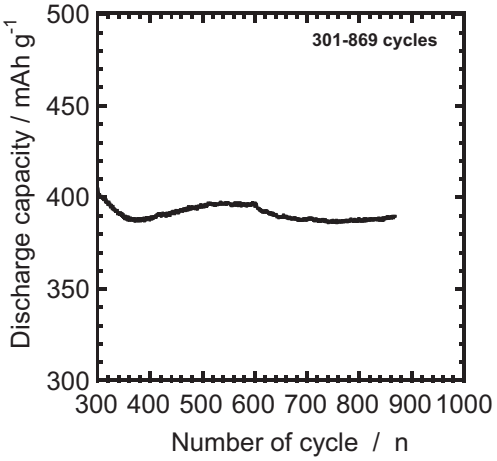

Fig. 5. Evolution of the discharge capacity of the cell at 5.8 mA (2.0 C) from 301 to 869 cycles. The waves around 600 cycles are due to technical sources. During these experiments, operations for measurement were stopped at the 600th cycle and resumed again after few hours.

3.3. Cyclic voltammetry

Fig. 6 shows the 10th cyclic voltammograms of the cell performed after 300 and 869 charge–discharge cycles at 5.0 mA and 5.8 mA, respectively. The corresponding numerical values are tabulated in Table 2. In both cases, unique redox couples with oxidation (anodic) peaks prior the oxygen evolution, E_a at 485 and 458 mV and reduction (cathodic) peaks, E_c at 338 and 301 mV on the reverse sweep are observed after 300 and 869 charge–discharge cycles, respectively. These peaks could be assigned to the γ-NOOH and α-$Ni(OH)_2$ reaction process. The uniqueness of these redox couples suggests that only the α/γ redox reaction occurs during the cycles. The potential difference between the anodic and cathodic peaks, $\Delta E_{a,c}$, is an important parameter to evaluate the electrochemical properties. It is taken to estimate the reversibility of the electrochemical redox reaction; the smaller $\Delta E_{a,c}$, the more reversible the electrochemical reaction and better proton diffusion efficiency [40]. From Fig. 6 and Table 2, the charge process appear to occur more reversibly with $\Delta E_{a,c}$ of 147 and 157 mV in both half cell conditions and battery regime, respectively. More importantly, a $\Delta E_{a,c}$ of 157 mV combined with the uniqueness of the redox couple

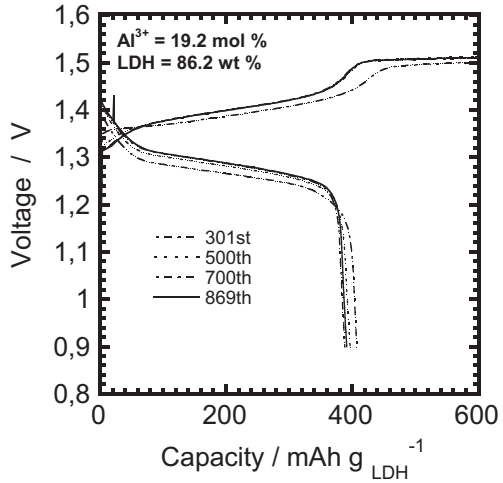

Fig. 4. Charge–discharge curves at 5.8 mA for the 301st, 500th, 700th and 869th cycles.

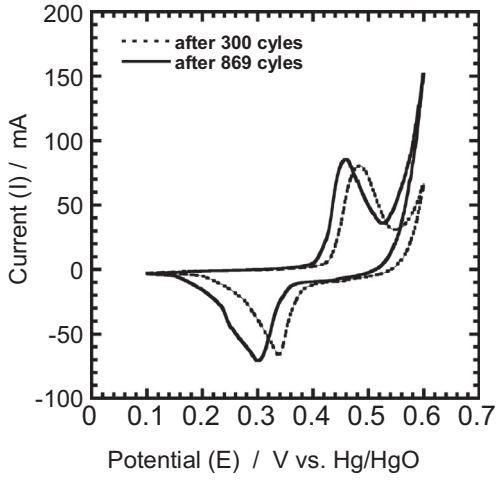

Fig. 6. 10th cyclic voltammograms of the cell after: (broken line) 300 cycles at 5.0 mA; (solid line) 869 cycles at 5.8 mA.

Table 2
Numerical values for the 10th cyclic voltammograms measured after 300 and 869 cycles, respectively.

Cell conditions	E_a (mV)	E_c (mV)	$\Delta E_{a,c}$ (mV)	DOP (mV)
After 300 cycles	485	338	147	115
After 869 cycles	458	301	157	142

obtained after more than 800 cycles confirms that the α/γ redox reaction has been maintained throughout all the cycles. These results indicate that cell still possesses an excellent electrochemical stability. On the other hand, the oxygen evolution is known as a parasitic reaction during charge on nickel electrode. The difference between the oxidation peak potential and the oxygen evolution potential (DOP) can be used to assess the charge efficiency of electrodes; an increase of oxygen evolution overpotential is beneficial to reduce the internal pressure of the battery [39]. According to Fig. 6, the peak potentials of the redox reaction appear at the less anodic potential (vs Hg/HgO), and DOP is higher (142 mV) in battery regime than in half cell conditions. These results show that the higher current (5.8 mA) is a suitable operating condition for the cathode. The shift of nickel hydroxide redox reaction to less anodic potentials and a higher DOP are known to be two major requirements for improvement in nickel battery electrodes [41]. The current studies illustrate that the LPD prepared Ni–Al LDH/C composites can satisfactorily be employed as cathode active materials for high performance Ni–MH batteries. The improvement of the electrochemical properties is attributed to the optimized composition during the materials preparation. The high discharge capacity implies high materials utilization [42]. These results are also in good agreement with those obtained by Corrigan et al. who have reported that coprecipitation of cobalt or manganese in nickel hydroxide thin films decreased the oxidation potential with regard to that of the unsubstituted nickel hydroxide [43].

The foregoing point out that the overall electrochemical performance of the LPD-based cathode materials is satisfactorily acceptable. In other words, the optimization of the synthetic conditions by using Ni:Al stoichiometry of 10:1 is an important issue since it results in the improved Ni–Al LDH/C composite with good crystallinity that allows the charge process to occur more easily and more reversibly. As we discussed in our previous work [25], the crystallinity basically depends on the LDH content, the higher the LDH content, the better the crystallinity. Furthermore, the optimal $Al^{3+}/(Al^{3+} + Ni^{2+})$ can be reached only at a higher LDH content. We believe that the good electrical connection provided with a current of 5.8 mA combined with both the optimal $Al^{3+}/(Al^{3+} + Ni^{2+})$ in the $Ni(OH)_2$ lattice and the LDH/carbon ratio in the composite can allow nickel hydroxide to be fully utilized during the charge, and nickel oxyhydroxide to be completely reduced during discharge [44,45]. As a result, a relatively great discharge capacity and a high utilization of active material can be achieved. The compositional diversity of chemical elements contained in the composite makes it difficult to unravel the kinetics of the nickel electrode oxidation/reduction processes, particularly because of the effects of additives and phase nonuniformities which are expected to provide additional kinetics and thermodynamic complexity. This aspect is beyond the scope of the present study whose main focus is the improvement of the synthetic conditions. Further investigations in order to clarify this assumption are necessary, and they will be addressed subsequently.

4. Conclusion

Ni–Al LDH/C composites fabricated by the LPD method have been successfully employed as cathode active materials for Ni–MH secondary battery. XRD patterns show peaks assigned to γ-NiOOH after charge, and Al-doped α-$Ni(OH)_2$ after discharge, indicating that the α/γ redox reactions occur without any intermediate phase. The sample prepared with Ni:Al stoichiometry of 10:1 exhibited good crystallinity, higher LDH content (86.2 wt%) as well as optimal $Al^{3+}/(Al^{3+} + Ni^{2+})$ of 19.2 mol%. Charging at 5 mA shows the good electrode stability, and therefore it is recommended for Ni–Al LDH/C composite active materials. The cell exhibits an excellent lifespan over 869 cycles of charge–discharge with the capacity retention above 380 mA h g_{comp}^{-1}. Cyclic voltammetry revealed that the cell possesses an excellent electrochemical stability, a good charge efficiency and an improved materials utilization. With further investigations on the metal-hydride (M – H) anode, Ni–Al LDH/C composites are expected to be applied as high rate discharge electrode materials in the next generation of Ni–MH secondary batteries.

Acknowledgments

This study was carried out as the Energy and Environment Technologies Development Projects; “Development of an Electric Energy Storage System for Grid-connection with New Energy Resources” supported by Kawasaki Heavy Industries Ltd., the New Energy and Industrial Technology Organization (NEDO), Grant-in-aid for Scientific Research (B) No. 22350094, and JSPS Japan. We are thankful to Ms. Hazuki Otsuka of Osaka Prefecture University for kind assistance during the experimental evaluation of the electrodes.

Appendix A. Supplementary data

Supplementary data related to this article can be found at http://dx.doi.org/10.1016/j.jpowsour.2013.08.001.

References

[1] M.M. Moorthi, in: Proceedings of the 28th Annual International Telecommunications Energy Conference, INTELEC ’06, IEEE Conference Publications, 2006, pp. 112–118.
[2] J.J.C. Kopera, Proceedings of the International Stationary Battery Conference, Battcon 2005 Conference, Miami Beach, Florida, USA.
[3] a) S. Terada, K. Higaki, E. Kitagawa, D. Kouzaki, I. Nagashima, E. Yoshiyama, K. Morimoto, K. Ishikawa, PRiME 2008 Meeting. Abs. No. 665, The Electrochemical Society, 2008;
b) K. Nishimura, T. Takasaki, T.Sakai, J. Alloys Compd., in press
[4] T. Takasaki, K. Nishimura, T. Mukai, T. Iwaki, K. Tsutsumi, T. Sakai, J. Electrochem. Soc. 159 (2012) A1891–A1896.
[5] H. Bode, K. Dehmelt, J. Wine, Electrochim. Acta 11 (1966) 1079–1087.
[6] D.A. Corrigan, S.L. Knight, J. Electrochem. Soc. 136 (1989) 613–619.
[7] C. Faure, C. Delmas, M. Fouassier, J. Power Sources 35 (1991) 279–290.
[8] F. Portemer, A. Delahaye-Vidal, M. Figlarz, J. Electrochem. Soc. 139 (1992) 671–678.
[9] P.V. Kamath, M. Dixit, L. Indira, A.K. Shukla, V.G. Kumar, N. Munichandraiah, J. Electrochem. Soc. 141 (1994) 2956–2959.
[10] V.G. Kumar, N. Munichandraiah, P.V. Kamath, A.K. Shukla, J. Power Sources 56 (1995) 111–114.
[11] R.D. Armstrong, E.A. Charles, J. Power Sources 25 (1989) 89–97.
[12] L.L. Demourgues-Guerlou, C. Delmas, J. Electrochem. Soc. 143 (1996) 561–566.
[13] L. Indira, M. Dixit, P.V. Kamath, J. Power Sources 52 (1994) 93–97.
[14] R.S. Jayashree, P.V. Kamath, J. Power Sources 107 (2002) 120–124.
[15] L.J. Yang, X.P. Gao, Q.D. Wu, H.Y. Zhu, G.L. Pan, J. Phys. Chem. C 111 (2007) 4614–4619.
[16] F. Yang, B.Y. Xie, J.Z. Sun, J.K. Jin, M. Wang, Mater. Lett. 62 (2008) 1302–1304.
[17] H. Nagayama, H. Honda, H. Kawahara, J. Electrochem. Soc. 135 (1988) 2012–2016.
[18] A. Hishinuma, T. Goda, M. Kitaoka, S. Hayashi, H. Kawahara, Appl. Surf. Sci. 48 (49) (1991) 405.
[19] S. Deki, Hnin Yu Yu Ko, T. Fujita, K. Akamatsu, M. Mizuhata, A. Kajinami, Eur. Phys. J. D 16 (2001) 325–328.
[20] S. Deki, S. Iizuka, A. Horie, M. Mizuhata, A. Kajinami, Chem. Mater. 16 (2004) 1747–1750.
[21] S. Deki, S. Iizuka, K. Akamatsu, M. Mizuhata, A. Kajinami, J. Am. Ceram. Soc. 88 (2005) 731–736.
[22] S. Deki, A. Hosokawa, A.B. Béléké, M. Mizuhata, Thin Films Solids 517 (2009) 1546–1554.
[23] M. Mizuhata, A. Hosokawa, A.B. Béléké, S. Deki, ECS Trans. 19 (2009) 41–46.

[24] A.B. Béléké, M. Mizuhata, J. Power Sources 195 (2010) 7669–7676.
[25] A.B. Béléké, E. Higuchi, H. Inoue, M. Mizuhata, J. Power Sources 225 (2013) 215–220.
[26] H. Maki, Y. Mori, Y. Okumura, M. Mizuhata, Mater. Chem. Phys. 141 (2013) 445–453.
[27] M.A. Kiani, M.F. Mousavi, S. Ghasemi, J. Power Sources 195 (2010) 5794–5800.
[28] A. Sugimoto, S. Ishida, K. Hanawa, J. Electrochem. Soc. 146 (1999) 1251–1255.
[29] L. Lei, M. Hu, X. Gao, Y. Sun, Electrochim. Acta 54 (2008) 671–676.
[30] S.-J. Kim, G.-J. Park, B.B. Kim, J.-K. Chung, G.G. Wallace, S.-Y. Park, Synth. Met. 161 (2012) 2641–2646.
[31] Z. Hengbin, L. Hanssan, C. Xuejing, L. Shujia, S. Chiachung, Mater. Chem. Phys. 79 (2003) 37–42.
[32] M. Hu, X. Gao, L. Lei, Y. Sun, J. Phys. Chem. C 113 (2009) 7448–7455.
[33] X.-Z. Fu, X. Wang, Q.-C. Xu, J. Li, J.-Q. Xu, J.-D. Lin, D.-W. Liao, Electrochim. Acta 52 (2007) 2109–2115.
[34] M. Hu, Z. Yang, L. Lei, Y. Sun, J. Power Sources 196 (2011) 1569–1577.
[35] C. Delmas, C. Faure, Y. Borthomieu, Mater. Sci. Eng. B13 (1992) 89–96.
[36] Y. Li, W. Li, S. Chou, J. Chen, J. Alloys Compd. 456 (2008) 339–343.
[37] Y.L. Zhao, J.M. Wang, H. Chen, T. Pan, J.Q. Zhang, C.N. Cao, Int. J. Hydrogen Energy 29 (2004) 889–896.
[38] W.K. Hu, X.P. Gao, D. Noréus, T. Burchardt, N.K. Nakstad, J. Power Sources 8 (1982) 229–255.
[39] Q.D. Wu, X.P. Gao, G.R. Li, G.L. Pan, T.Y. Yan, H.Y. Zhu, J. Phys. Chem. C 111 (2007) 17082–17087.
[40] D.A. Corrigan, R.M. Bandert, J. Electrochem. Soc. 136 (1989) 723–728.
[41] B. Liu, Z. Yunshi, H. Yuan, H. Yang, E. Yang, Int. J. Hydrogen Energy 25 (2000) 333–337.
[42] D. Bélanger, G. Laperrière, J. Electrochem. Soc. 137 (1990) 2355–2361.
[43] N. Sac-Epée, M.R. Palacin, B. Beaudoin, A. Delahaye-Vidal, T. Jamin, Y. Chabre, J.M. Tarascon, J. Electrochem. Soc. 144 (1997) 3896–3907.
[44] D.M. MacArthur, J. Electrochem. Soc. 117 (1970) 729–733.
[45] J.W. Weidner, P. Timmerman, J. Electrochem. Soc. 141 (1994) 346–351.